



Contents lists available at ScienceDirect

Free Radical Biology & Medicine

journal homepage: www.elsevier.com/locate/freeradbiomed

Original Contribution

Systemic administration of PEP-1–SOD1 fusion protein improves functional recovery by inhibition of neuronal cell death after spinal cord injury

Tae Young Yune^{a,*}, Jee Youn Lee^a, Mei Hua Jiang^a, Dae Won Kim^b, Soo Young Choi^b, Tae Hwan Oh^a^a Age-Related and Brain Diseases Research Center, Kyung Hee University, Seoul 130-701, Korea^b Department of Biomedical Science and Research Institute for Bioscience and Biotechnology, Hallym University, Chunchon 200-702, Korea

ARTICLE INFO

Article history:

Received 2 April 2008

Revised 19 June 2008

Accepted 15 July 2008

Available online xxx

Keywords:

Antioxidant enzymes

Motor neuron death

Neuroprotection

Peptide carrier

Reactive oxygen species

Spinal cord injury

ABSTRACT

Spinal cord injury (SCI) produces excessive levels of reactive oxygen species (ROS) that induce apoptosis of neurons. Cu,Zn-superoxide dismutase (SOD1) is a key antioxidant enzyme that detoxifies intracellular ROS, thereby protecting cells from oxidative damage. PEP-1 is a peptide carrier capable of delivering full-length native peptides or proteins into cells. In the study described here, we fused a human SOD1 gene with PEP-1 in a bacterial expression vector to produce a genetic in-frame PEP-1–SOD1 fusion protein; we then investigated the neuroprotective effect of the fusion protein after SCI. The expressed and purified PEP-1–SOD1 was efficiently delivered into cultured cells and spinal cords *in vivo*, and the delivered fusion protein was biologically active. Systemic administration of PEP-1–SOD1 significantly decreased levels of ROS and protein carbonylation and nitration in spinal motor neurons after injury. PEP-1–SOD1 treatment also significantly inhibited mitochondrial cytochrome c release and activation of caspase-9 and caspase-3 in spinal cords after injury. Furthermore, PEP-1–SOD1 treatment significantly reduced ROS-induced apoptosis of motor neurons and improved functional recovery after SCI. These results suggest that PEP-1–SOD1 may provide a novel strategy for the therapeutic delivery of antioxidant enzymes that protect neurons from ROS after SCI.

© 2008 Elsevier Inc. All rights reserved.

Neuronal cell death following traumatic spinal cord injury (SCI) is a delayed process that contributes to progressive secondary degeneration and, ultimately, results in spinal cord dysfunction below the injury site [1–4]. This secondary neuronal death stems, in part, from the deleterious substances produced in response to the primary insult [2,5,6]. Among these substances are reactive oxygen species (ROS), which are produced excessively and contribute to neuronal death after SCI [2,3,7–9]. ROS initiate chain reactions and damage cellular macromolecules, including proteins, DNA, and membrane phospholipids, thereby causing cell death. Aside from this direct damage, ROS have been shown to induce mitochondrial cytochrome c release followed by activation of caspases, leading to apoptotic cell death of neurons after SCI [3,7–11]. Several endogenous antioxidant enzymes, such as superoxide dismutases (SODs), glutathione peroxidases, and catalase, can detoxify ROS; however, overproduction of ROS after

injury often exceeds the capacity of these enzymes, causing oxidative stress and subsequent cell death.

Ventral horn motor neurons (VMNs) are selectively vulnerable to acute SCI [12] and to neurodegenerative diseases such as amyotrophic lateral sclerosis (ALS) [13,14]. Recent reports indicate that increased production of ROS after SCI contributes to motor neuron death [15], whereas overexpression of SOD1 protects VMNs from ROS [11]. Furthermore, oxidative stress has been implicated in the pathogenesis of selective motor neuron death in animal models of SCI and familial ALS [16,17]. For example, mitochondrial cytochrome c release into cytosol and concomitant caspase-9 activation occur in the spinal motor neurons of mutant SOD1 mice in parallel with the neurodegenerative process [17].

A series of small protein domains, called protein transduction domains (PTDs; e.g., Tat protein from HIV-1, the third α -helix of *Antennapedia* homeodomain, and VP22 protein from herpes simplex virus), have been shown to cross plasma membranes efficiently and to promote delivery of peptides and proteins into cells [18–20]. Recently, a 21-residue peptide carrier, PEP-1, was developed as a tool for delivering biologically active molecules into cells [21]. It consists of three domains: a hydrophobic tryptophan-rich motif (KETW-WETWWTEW), a spacer domain (SQP), and a hydrophilic lysine-rich domain (KKKRKV). This peptide carrier allows the delivery of a variety of peptides and proteins into cells in a biologically active form, without the need for crosslinking or denaturation steps [21]. A recent

Abbreviations: SCI, spinal cord injury; ROS, reactive oxygen species; ALS, amyotrophic lateral sclerosis; BBB, Basso–Beattie–Bresnahan; Cy5.5, Cy 5.5 NHS ester; FITC, fluorescein isothiocyanate; HET, hydroethidine; 5-HT, 5-hydroxytryptamine; NF, neurofilament; PTD, protein transduction domain; SDS–PAGE, sodium dodecyl sulfate–polyacrylamide gel electrophoresis; SOD, superoxide dismutase; TUNEL, terminal deoxynucleotidyl transferase dUTP nick end labeling; VMN, ventral horn motor neuron.

* Corresponding author. Kyung Hee University, Age-Related and Brain Diseases Research Center, Medical Building 10th Floor, Dongdaemun-gu, Hoegi-dong 1, Seoul 130-701, Republic of Korea. Fax: +82 02 969 6343.

E-mail address: tyune@khu.ac.kr (T.Y. Yune).

0891-5849/\$ – see front matter © 2008 Elsevier Inc. All rights reserved.

doi:10.1016/j.freeradbiomed.2008.07.016

Please cite this article as: Yune, T. Y.; et al., Systemic administration of PEP-1–SOD1 fusion protein improves functional recovery by inhibition of neuronal cell death after spinal cord injury, *Free Radic. Biol. Med.* (2008), doi:10.1016/j.freeradbiomed.2008.07.016

report indicates that systemic injection of PEP-1–SOD1 fusion protein prevents neuronal cell death in the hippocampus caused by transient forebrain ischemia and paraquat-induced dopaminergic neuron damage in a Parkinson disease mouse model [22,23].

In the study described here, we demonstrated that PEP-1–SOD1 can be delivered efficiently into the injured spinal cord, protects motor neurons from ROS, and improves functional recovery after SCI. Therefore, we suggest that PEP-1–SOD1 may represent a potential therapeutic agent for treatment of acute SCI.

Materials and methods

Expression and purification of PEP-1–SOD1 fusion protein

Construction of PEP-1–SOD1 (human Cu,Zn-SOD) expression vector, expression of PEP-1–SOD1 in *Escherichia coli*, and purification of the expressed enzyme have been described [22].

Spinal cord injury

Adult rats (Sprague–Dawley, male, 250–300 g; Sam: TacN(SD)BR; Samtako, Osan, Korea) were anesthetized with chloral hydrate (500 mg/kg, ip), and a laminectomy was performed at the T9–10 level, exposing the cord beneath without disrupting the dura. The spinous processes of T8 and T11 were then clamped to stabilize the spine, and the exposed dorsal surface of the cord was subjected to contusion injury (10 g×25 mm) using a NYU impactor as previously described [24]. Sham-operated controls underwent a T10 laminectomy without weight-drop injury. All surgical interventions and postoperative animal care were in accordance with the Guidelines and Policies for Rodent Survival Surgery provided by the Animal Care Committee of Kyung Hee University.

Primary cortical neuron cultures

Primary cortical neuron cultures were prepared from the cerebral cortices of embryonic 16-day Sprague–Dawley rats (Samtako) according to the protocol described previously [25]. Briefly, cerebral cortices removed with meninges were dissected in Hanks' balanced saline solution (Invitrogen, Carlsbad, CA, USA), dissociated by trypsinization followed by trituration, and passed through a 210- μ m nylon mesh (Sefar America, Kansas City, MO, USA). Neurons were plated on poly-D-lysine (20 μ g/ml)-coated six-well plates (3×10^5 cells/well) or glass coverslips in a 24-well plate (4×10^4 cells/well), and maintained in neurobasal medium (Invitrogen) supplemented with B27 (Invitrogen) and 0.5 mM glutamine in a humidified 5% CO₂ incubator at 37°C. Culture medium was replaced with fresh medium every 2 days for 1 week, and cells were then used.

Delivery of PEP-1–SOD1 into cultured neurons and injured spinal cords

To examine whether PEP-1–SOD1 can be delivered into cells in vitro and in vivo, the purified PEP-1–SOD1 was labeled with FITC (Pierce, Rockford, IL, USA) or Cy 5.5 NHS ester (Cy5.5) (GE Healthcare, Little Chalfont, UK) according to the manufacturer's instructions. FITC- or Cy5.5-labeled SOD1 was used as a control. For detection of PEP-1–SOD1 protein delivered into cells, cultured neurons were treated with 2 μ M FITC- or Cy5.5-labeled PEP-1–SOD1 or SOD1 for 30 min, washed, and then fixed with 4% paraformaldehyde. Cells were observed and photographed with an Olympus microscope with software accompanying the Cool SNAP camera (Roper Scientific, Tucson, AZ, USA). The intracellular stability of delivered PEP-1–SOD1 was then examined in the following manner. Cells were treated with 2 μ M PEP-1–SOD1 for 30 min, washed, and changed with a fresh culture medium. Then, cells were further incubated for the time indicated, followed by preparations of cell extracts for Western blot analysis. For detection of PEP-1–

SOD1 delivered into injured spinal cords, Cy5.5-labeled PEP-1–SOD1 or SOD1 (1 mg/rat) was injected intraperitoneally immediately after injury. One day after injection, spinal cord tissues were prepared as previously described [24], and the fluorescence was monitored by molecular real imaging using an Imaging Station 4000MM (Kodak, Rochester, NY, USA). Some spinal cord sections were processed for immunohistochemical staining using specific cell type makers: NeuN for neurons; CC1 for oligodendrocytes; OX42 for microglia; and glial fibrillary acidic protein for astrocytes as described below.

Administration of PEP-1–SOD1

PEP-1–SOD1 was dissolved in sterile phosphate-buffered saline and injected intraperitoneally into animals randomly assigned to either control or treatment groups as follows: for hydroethidine (HET) detection and SOD activity ($n=3$ for each SOD1 or PEP-1–SOD1); for Western blot, DNA laddering, protein carbonylation, and caspase-3 activity ($n=3$ for each sham-operated, SOD1 or PEP-1–SOD1); for TUNEL, cresyl violet, 5-HT, and neurofilament (NF200) staining and lesion area analysis ($n=5$ for each SOD1 or PEP-1–SOD1); and for behavioral testing ($n=25$ for each SOD1 or PEP-1–SOD1). Rats were given PEP-1–SOD1 (1 mg/rat) immediately after injury and then received 1 mg/rat PEP-1–SOD1 intraperitoneally every 24 h for 3 consecutive days. The control group received intraperitoneal injections of SOD1. A previous article reported that 4 mg/kg PEP-1–SOD1 is an optimal dose for neuroprotection after ischemic insult [22]. For determination of the therapeutic time windows of PEP-1–SOD1, rats were injected with PEP-1–SOD1 (1 mg/rat) 2, 4, or 8 h after SCI and then were injected with 1 mg/rat PEP-1–SOD1 intraperitoneally every 24 h for 3 consecutive days ($n=12$ for each time point).

Enzyme activity assay of SOD1

After SCI, PEP-1–SOD1 (1 mg/rat) was injected intraperitoneally, and spinal cords were taken 1 day after injury. SOD1 activity was measured using a SOD enzyme assay kit (Calbiochem, San Diego, CA, USA) as previously described [26]. The amount of SOD1 required to inhibit the rate of reduction of cytochrome c by 50% was defined as 1 unit of activity.

In situ detection of superoxide anion

The production of O₂⁻ after SCI was examined by the in situ detection of oxidized HET using HET dye (Invitrogen). HET is oxidized to the fluorescent ethidium by O₂⁻ [28,29] and is considered an indicator of intracellular O₂⁻ [26]. Two hundred microliters of HET (1 mg/ml in phosphate-buffered saline) was injected intravenously 1 h before the animals were killed. Animals were killed 4 h after injury, and spinal cord sections were prepared as previously described [24]. Fluorescence was assessed microscopically at excitation=355 nm and emission >415 nm for HET detection, or at excitation=510–550 nm and emission >580 nm for ethidium detection and photographed with an Olympus microscope with software accompanying the Cool SNAP camera. For quantitative analysis of ethidium fluorescence, the area of tissue fluorescence in three coronal sections in each animal was analyzed using Image MetaMorph software (Molecular Devices, Sunnyvale, CA, USA) as described previously [11].

Western blot

Segments of spinal cord (1 cm) were isolated using the lesion site as the epicenter, and spinal cord tissues were homogenized in a lysis buffer containing 1% Nonidet P-40, 20 mM Tris, pH 8.0, 137 mM NaCl, 0.5 mM EDTA, 10% glycerol, 10 mM Na₂P₂O₇, 10 mM NaF, 1 μ g/ml aprotinin, 10 μ g/ml leupeptin, 1 mM vanadate, and 1 mM phenylmethylsulfonyl fluoride. Tissue homogenates were incubated for

20 min at 4°C and centrifuged at 25,000 g for 30 min at 4°C. The protein level of the supernatant was determined using the BCA assay (Pierce, Rockford, IL, USA). Protein extraction of both the mitochondrial and cytosolic fractions was performed 4 h after SCI as previously described [27]. Total or cytoplasmic (S-100) (50 µg) and mitochondrial (10 µg) protein was separated by SDS-PAGE and transferred to nitrocellulose membranes (Millipore, Billerica, MA, USA) by electrophoresis. The membranes were then incubated with polyclonal antibodies against cytochrome c, caspase-9 (1:1000, Santa Cruz Biotech, Santa Cruz, CA, USA), nitrotyrosine (Millipore), and caspase-3 (1:1000, Cell Signaling, Danvers, MA, USA). The membranes were processed with horseradish peroxidase-conjugated secondary antibody (Jackson Laboratories). Immunoreactive bands were visualized by chemiluminescence using Supersignal (Pierce). Experiments were repeated three times to ensure reproducibility. Western blot analysis of protein carbonylation was performed according to the protocol of the OxyBlot Protein Oxidation Detection Kit (Millipore). Tubulin was used as an internal control. Relative intensity of each band on Western blots and carbonylated proteins were measured and analyzed with Alphamager software (Alpha Innotech Corporation, San Leandro, CA, USA). Background in films was subtracted from the optical density measurements.

Caspase-3 activity

Caspase-3 enzyme activity was assayed 4 h after injury as previously described [24]. Briefly, segments of spinal cord (1 cm) including the lesion site were isolated and homogenized in homogenization buffer as previously described [24]. One hundred micrograms of protein was added to 1 ml of homogenization buffer containing 15 µM Z-DEVD-AFC (Enzyme Systems Products, Livermore, CA, USA). Samples were incubated at room temperature for 5 min, and relative fluorescence (excitation at 400 nm and emission at 505 nm) was measured for 1 h using a fluorescence microplate reader (Molecular Devices). The specific activity of the samples was calculated relative to a standard curve using recombinant caspase-3 (Millipore).

Cell counting of viable VMNs

Four days after injury, we assessed the number of VMNs. The criteria for VMN counting described by Sugawara et al. [11] were used. In brief, we determined the cells located in the lower ventral horn larger than half of the sampling square (20×20 µm) as VMNs. Cells above the line at 150 µm ventral from the central canal were excluded. To determine the total number of VMNs, we stained serial transverse sections (20-µm thick) with cresyl violet acetate and counted at an interval of approximately 500 µm within 2.5 mm of the center of the lesion, for a total of 11 sections from each animal. The cells from each field were manually counted using Metamorph software (Molecular Devices).

TUNEL and immunohistochemical staining

One day after injury, serial coronal spinal cord sections (10 µm thick) were collected, and every 50 µm sections were processed for TUNEL and then for immunohistochemistry using a neuron-specific marker, NeuN (1:1000, Millipore), as previously described [24]. Only double-labeled cells (TUNEL+NeuN) were considered and counted as TUNEL-positive neurons in the gray matter (from centromedial to ventral region) extending from 2 mm rostral to 2 mm caudal to the lesion epicenter from each section. Some sections were processed for immunohistochemistry using antibody against nitrotyrosine (1:1000, Millipore). Also, nuclei were labeled with 4',6'-diamidino-2-phenylindole according to the protocol of the manufacturer (Invitrogen). Serial sections were also stained with cresyl violet acetate. For quantitative analysis of axonal densities, serial coronal sections collected every

millimeter rostral and caudal 3 mm to the lesion site from spinal tissues used for the behavioral test were stained with NF200 (1:4000, Sigma). Some sections were processed for 5-HT (1:5000, Diasorin, Stillwater, MN, USA) staining. Sections were examined with the 40× objective of the microscope, and digital images were captured with a Cool SNAP camera. Axonal densities were determined within preselected fields (40×40 µm, 1600 µm²), at specific sites within the ventral and dorsolateral funiculi. The location of these sites was carefully conserved from group to group using anatomical landmarks, and NF200-stained axons from each field were manually counted using Metamorph software. The number of axons in SOD1- or PEP-1-SOD1-treated spinal cord was expressed as a percentage relative to that in sham controls (100%).

DNA laddering

Segments of spinal cord (1 cm) were isolated using the lesion site as the epicenter at 1 day after SCI, and DNA was separated by electrophoresis as previously described [24].

Behavioral tests

Examination of functional deficits after injury was conducted as previously described [24]. Behavioral analyses were performed by trained investigators who were blind to the experimental conditions. To test hindlimb locomotor function, open-field locomotion was evaluated using the Basso-Beattie-Bresnahan (BBB) locomotion scale as previously described [30,31]. The BBB scale is a 22-point scale (scores 0–21) that systematically and logically follows recovery of hindlimb function from a score of 0, indicative of no observed hindlimb movements, to a score of 21, representative of a normal ambulating rodent. An inclined plane test was performed according to the method described by Rivlin and Tator [32]. In brief, animals were tested in two positions (right side or left side up) on the testing apparatus (i.e., a board covered with a rubber mat containing horizontal ridges spaced 3 mm apart). The maximum angle at which a rat could maintain its position for 5 s without falling was recorded for each position, and these were averaged to obtain a single score for each animal. The ability to control and place the hindlimb precisely was tested on a horizontal grid as previously described [33]. Analysis was performed by counting the number of footfalls (mistake) in foot placing. Footprint analysis was performed as previously described [34]. Both the animal's forepaws and hindpaws were dipped in red and blue dye (nontoxic) and then walked across a narrow box (1 m long and 7 cm wide). The footprints were scanned, and digitized images were analyzed.

Assessment of lesion volume

The measurement of lesion volume using rats tested for behavioral analysis was performed as described previously [24,30]. Serial longitudinal sections (10 µm) through the dorsoventral axis of the spinal cord were used to determine lesion volume. Every 50 µm sections were stained with cresyl violet acetate and studied with light microscopy. The rostrocaudal boundaries of the tissue damage were defined by the presence of inflammatory cells, the loss of neurons, the existence of degenerating neurons, and cyst formation. With a low-power (1.25×) objective, the lesion area was determined with MetaMorph software. Areas at each longitudinal level were determined, and the total lesion volume was derived by means of numerical integration of sequential areas.

Statistical analysis

Data are presented as mean±SD values. Quantitative data from behavioral tests were evaluated for statistical significance using two-

way ANOVA with a post hoc Tukey test; data from enzyme activity assay, TUNEL-positive cells, VMN counting, lesion volume, axons, and Western blot analyses were evaluated for statistical significance using Student's paired *t* test. In all analyses, a *P* value <0.05 was considered statistically significant.

Results

PEP-1-SOD1 is delivered efficiently into cultured neurons and injured spinal cord tissues

PEP-1-SOD1 was expressed and purified and then confirmed by Western blot as previously described [22,23] (Figs. 1A and B). To investigate its delivery into living cells and spinal cords, PEP-1-SOD1 was labeled with FITC or Cy5.5 fluorescence dye. Data show that FITC- or Cy5.5-labeled PEP-1-SOD1 was delivered into cultured neurons, whereas neither FITC- nor Cy5.5-labeled SOD1 (control) was delivered into the cells (Fig. 1C). Furthermore, Western blot analysis revealed that PEP-1-SOD1 fusion protein was rapidly delivered into cells, and the intracellular stability of delivered PEP-1-SOD1 persisted for 24 h, whereas SOD1 (control) was not delivered into cells (Fig. 1D). When Cy5.5-labeled PEP-1-SOD1 (1 mg/rat) was injected intraperitoneally into rats after SCI, the fusion protein was delivered into spinal cord tissues as revealed by a molecular real imaging technique (Fig. 1E). Furthermore, immunohistochemical staining revealed that Cy5.5-

labeled PEP-1-SOD1 was detected in neurons, oligodendrocytes (Fig. 1F), astrocytes, and microglia (data not shown). To determine whether PEP-1-SOD1 delivered into spinal cords was biologically active, we measured SOD1 enzyme activities in total extracts of spinal cord tissues 1 day after PEP-1-SOD1 injection. The specific SOD activities of PEP-1-SOD1-treated spinal cords were significantly higher than those of SOD1-treated cords (Fig. 1G).

PEP-1-SOD1 alleviates ROS after SCI

We investigated the effect of PEP-1-SOD1 on the level of ROS after SCI using HET, a fluorescent dye that is a specific indicator of superoxide anion ($O_2^{\cdot-}$). Strong HET fluorescence was observed in the cytoplasm of VMNs and interneurons after SCI, whereas no fluorescence was observed in these neurons in the sham-operated spinal cord (Fig. 2A). On higher magnification, strong HET fluorescence in VMNs appeared as punctations in the cytoplasm (Fig. 2A, right bottom panel), suggesting the presence of $O_2^{\cdot-}$ in mitochondria as reported [11]. When PEP-1-SOD1 was injected into the rat after SCI, the number of HET-positive VMNs and the intensity of fluorescence decreased when compared with the SOD1-treated control (Fig. 2A). Quantitative analysis showed that the relative intensity of ethidium fluorescence in the PEP-1-SOD1-treated spinal cord was significantly lower than that in the SOD1-treated cord 4 h after injury (Fig. 2B).

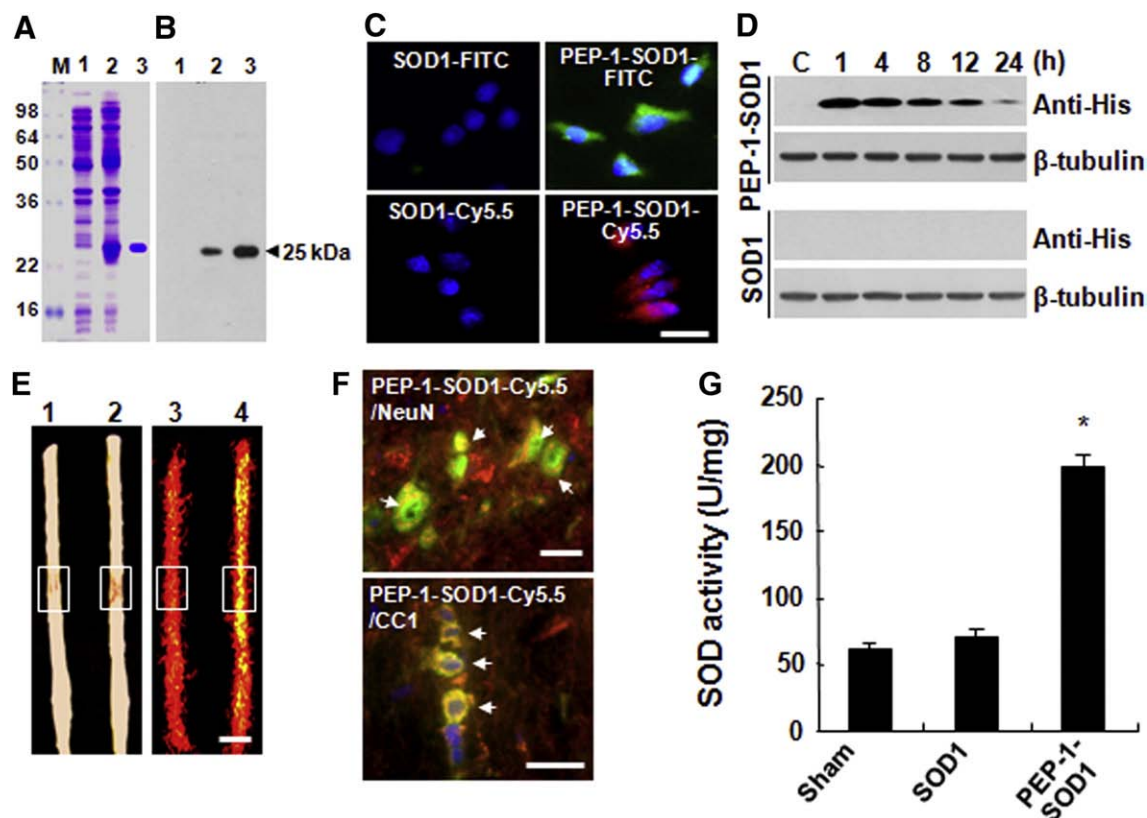


Fig. 1. PEP-1-SOD1 fusion protein was delivered into primary cultured neurons and injured spinal cord. Coomassie blue staining of SDS-PAGE of induced PEP-1-SOD1 protein extracts and purified fusion protein (A) and Western blot (B) using an anti-rabbit polyhistidine antibody. Lane M, molecular weight standards; lane 1, not induced; lane 2, induced; lane 3, purified PEP-1-SOD1. (C) Cellular localization of FITC- or Cy5.5-labeled PEP-1-SOD1 or SOD1 (control) in primary cortical neuron culture. Primary neurons were treated with 2 μ M FITC- or Cy5.5-labeled PEP-1-SOD1 or SOD1 for 30 min. Bar, 10 μ m. (D) Western blot analysis of the stability of PEP-1-SOD1 protein delivered into cultured neurons using an anti-rabbit polyhistidine antibody. Cultured neurons were incubated with 2 μ M PEP-1-SOD1 and control SOD1 for 30 min, and Western blotting was performed as described under Materials and Methods. (E) Real imaging of Cy5.5-labeled PEP-1-SOD1 delivered into the injured spinal cord. Lanes 1 and 2, brightfield images of SOD1- and PEP-1-SOD1-treated spinal cords, respectively; lanes 3 and 4, fluorescence images of Cy5.5-labeled SOD1- and PEP-1-SOD1-treated spinal cords, respectively. Insets indicate the lesion sites. Bar, 5 mm. (F) Detection of Cy5.5-labeled PEP-1-SOD1 protein (red) delivered into neurons (NeuN; green, arrows in upper panel) and oligodendrocytes (CC1; green, arrows in bottom panel) of the injured spinal cord. Sections were selected 2 mm rostral to the lesion site. Bar, 20 μ m. (G) The enzyme activity of SOD1 in total extracts of spinal cords 1 day after PEP-1-SOD1 injection. Data represent the means \pm SD obtained from three separate experiments. **P* < 0.05.

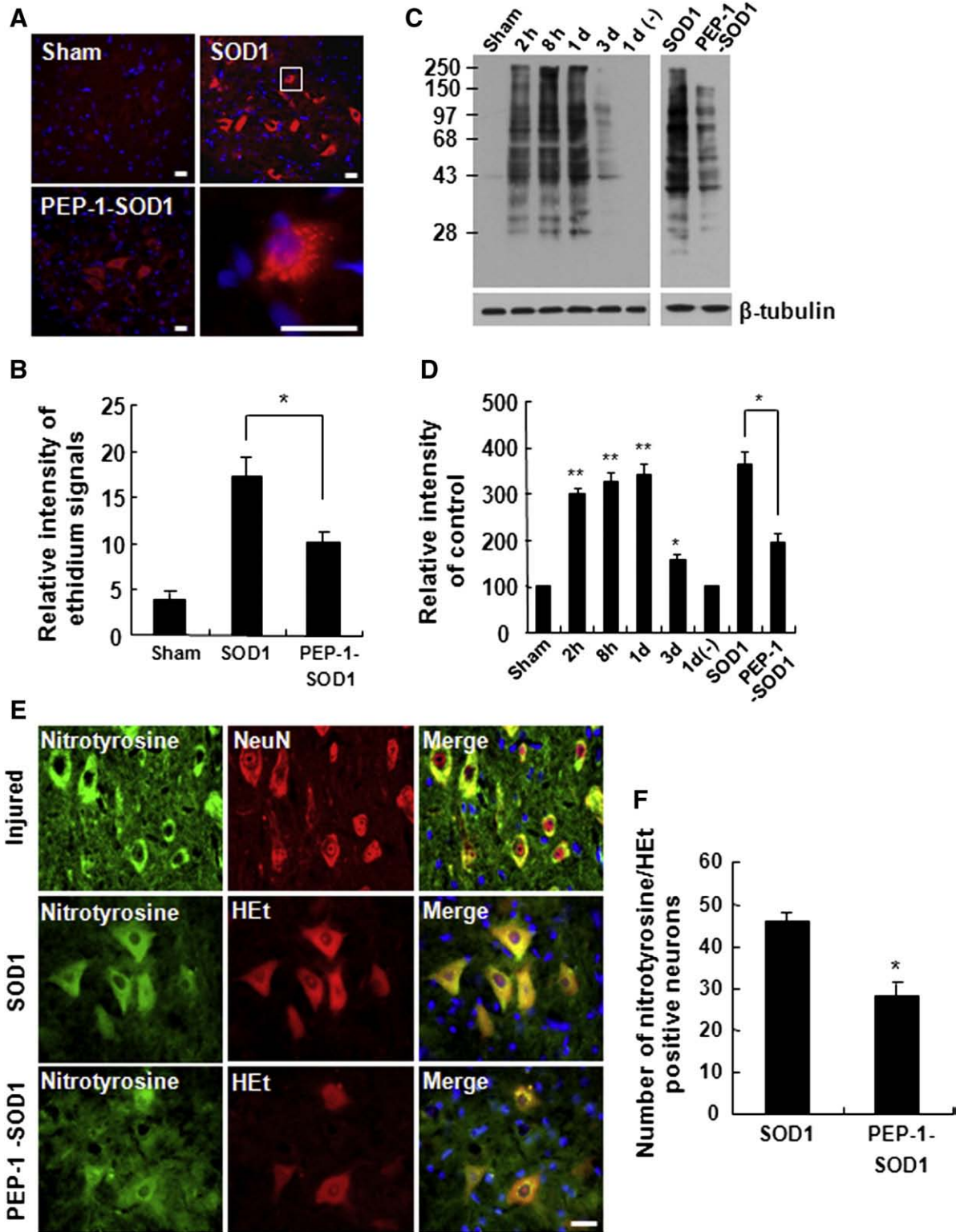


Fig. 2. PEP-1-SOD1 reduces superoxide anion and protein carbonylation and nitration after SCI. (A) Representative photomicrographs of HET fluorescence in spinal cord neurons. Two hundred microliters of HET (1 mg/ml in phosphate-buffered saline) was injected intravenously 1 h before the animals were killed. Animals were then killed at 4 h after injury, and spinal cord tissues were harvested. The right, bottom panel shows a VMN in the SOD1 control (inset) at higher magnification. Sections were taken 2 mm rostral to the lesion epicenter. Bars, 30 μ m. (B) Relative ethidium fluorescence intensity in spinal cords 4 h after injury. Fluorescence intensity was measured from the spinal cord sections taken 2 mm rostral to the lesion epicenter. Data represent the means \pm SD obtained from three experiments. * P < 0.05. (C) Temporal profiles of protein carbonylation after SCI. Lane 1 d (-) is a negative control in which carbonylated proteins were not detected on the membranes without 2,4-dinitrophenylhydrazine (DNPH) derivatization 1 day after injury. (D) Quantitative analysis of oxidatively modified proteins shows that PEP-1-SOD1 treatment significantly inhibits protein carbonylation when compared with the SOD1 control 1 day after injury. Values are means \pm SD of three separate experiments. * P < 0.05, ** P < 0.01. (E) Immunohistochemical analysis of protein nitration in VMNs 1 day after SCI. Note that a number of nitrotyrosine-positive neurons were observed in the ventral horn (nitrotyrosine; green, NeuN; red in upper panel). The nitrotyrosine immunoreactivity co-localized with HET in VMNs (nitrotyrosine; green, HET; red in middle and bottom panels). (F) For quantification, serial transverse sections (20 μ m thick) were collected every 500 μ m from 2.5 mm rostral to 2.5 mm caudal to the lesion epicenter (total of 11 sections) and nitrotyrosine/HET-positive neurons (>30 μ m in diameter) were counted. The coronal sections were taken 2 mm rostral to the lesion epicenter. Bar, 40 μ m.

PEP-1-SOD1 inhibits protein nitration and carbonylation after SCI

ROS induce damage to macromolecules such as proteins, lipids, and DNA, resulting in functional impairment of these molecules [35]. In particular, proteins are liable to be carbonylated and nitrosylated on tyrosine residues by ROS [36,37]. We examined the extent of protein carbonylation by ROS in the spinal cord as an index of protein oxidation after SCI. Carbonylated proteins were barely detectable in the sham control (Fig. 2C). By contrast, carbonylated proteins varying in molecular weight from 28 to 250 kDa were observed in the spinal cord after injury, and the extent of protein carbonylation gradually increased until 1 day after injury (Figs. 2C and D). However, PEP-1-SOD1 treatment markedly decreased protein carbonylation when compared with the SOD1 control (Figs. 2C and D). The levels of NO and peroxynitrite formed by the reaction between NO and O_2^- are increased after SCI [4,5]. As a strong oxidant, peroxynitrite can damage biological macromolecules such as protein, DNA, and membrane lipids [3,7–11]. For example, peroxynitrite induces nitrosylation of tyrosine

residues of proteins. To determine the effect of PEP-1-SOD1 on protein nitration, we performed immunohistochemistry by using specific antibody for nitrotyrosine 1 day after SCI. A number of nitrotyrosine-positive neurons were observed in the ventral horn of the injured spinal cord (Fig. 2E), whereas nitrotyrosine-positive neurons were not observed in the sham-operated spinal cord (data not shown). Nitrotyrosine-positive motor neurons in the ventral horn were also positive for HET fluorescent dye in both the SOD1 control and the PEP-1-SOD1-treated spinal cord (Fig. 2E), indicating co-localization of nitrated proteins and O_2^- in the neurons. Furthermore, PEP-1-SOD1 treatment decreased the number of nitrotyrosine/Het-positive motor neurons in ventral horn (Figs. 2E and F).

PEP-1-SOD1 inhibits cytochrome c release and activation of caspase-9 and caspase-3 after SCI

Mitochondrial cytochrome c release and caspase-3 activation occur at an early stage of apoptotic cell death after SCI [38,39]. As ROS have

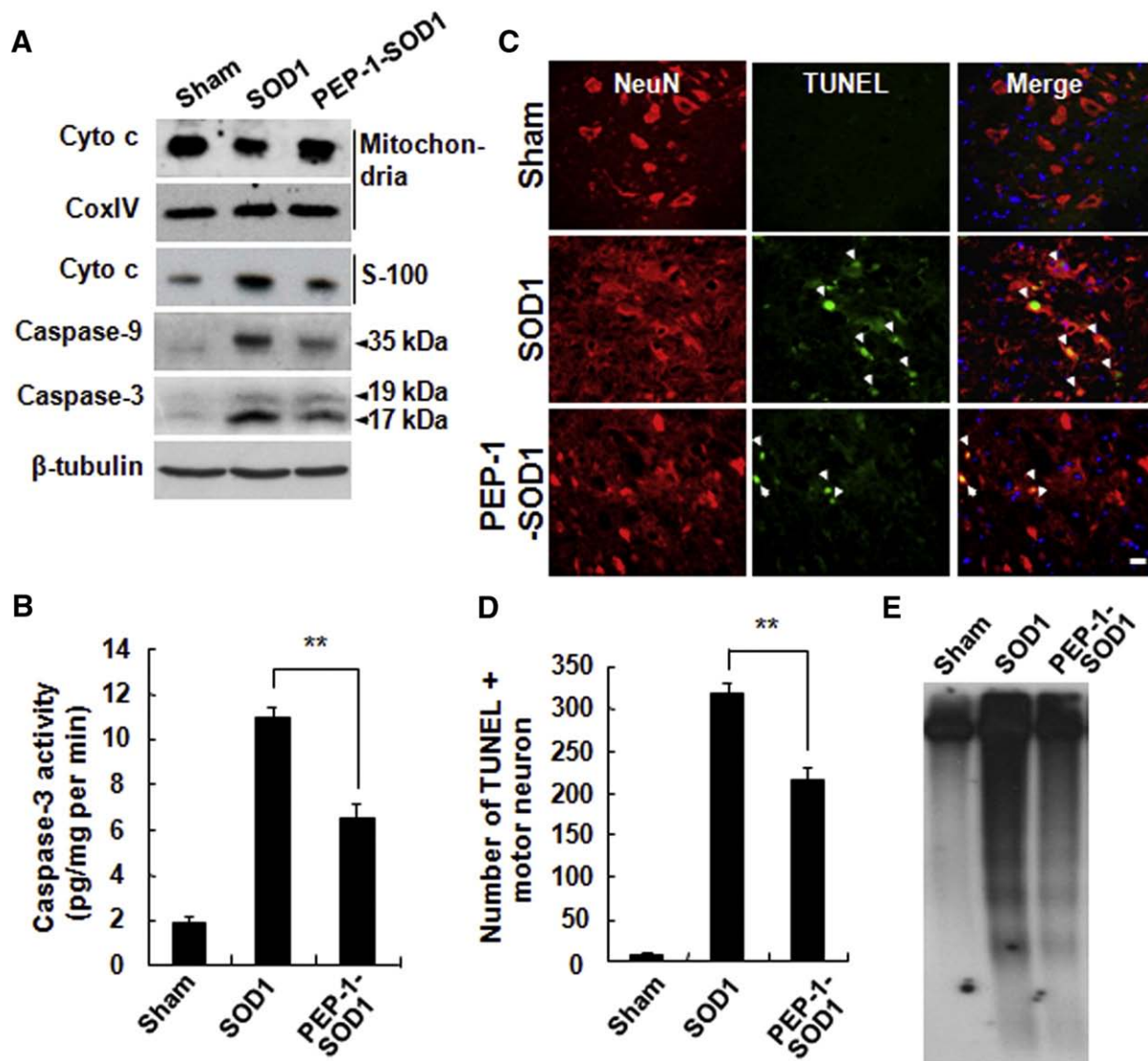


Fig. 3. PEP-1-SOD1 inhibits cytochrome c release, caspase activation, and motor neuron death after SCI. (A) The level of cytochrome c in mitochondrial and cytoplasmic fractions, and activation of caspase-9 and -3 4 h after injury. Cytochrome c oxidase (COXIV) was used as an internal control for mitochondrial fractions. (B) Caspase-3 activity in spinal cords 4 h after injury. Data represent the means \pm SD obtained from three separate experiments. $**P < 0.001$. (C) TUNEL of neurons in the ventral horn area 1 day after injury. Representative images were from the sections selected 1 mm rostral to the lesion epicenter. Arrows indicate TUNEL-positive neurons (TUNEL; green, NeuN; red). Bar, 40 μ m. (D) Quantitative analysis of TUNEL-positive neurons after injury. For quantification, serial transverse sections (20 μ m thick) were collected every 100 μ m section from 2 mm rostral to 2 mm caudal to the lesion epicenter (total of 40 sections), and the double (NeuN + TUNEL) positive neurons $> 30 \mu$ m in diameter in the ventral horn area of each section were counted. Data represent means \pm SD obtained from five separate experiments. $**P < 0.001$. (E) DNA gel electrophoresis of spinal cords 1 day after injury. $**P < 0.001$.

been implicated in inducing apoptotic cell death of VMNs after SCI [11], we anticipated that PEP-1–SOD1 treatment would inhibit mitochondrial cytochrome c release and caspase activation after SCI. Cytochrome c release into cytoplasm was markedly increased 4 h after SCI, and its release was noticeably attenuated by PEP-1–SOD1 treatment (Fig. 3A). Also, Western blot analyses revealed that the levels of cleaved (activated) forms of caspase-9 and caspase-3 were decreased by PEP-1–SOD1 treatment after injury (Fig. 3A), indicating that PEP-1–SOD1 treatment inhibits activation of caspase-9 and caspase-3. In addition, the specific caspase-3 activity in the PEP-1–SOD1-treated spinal cord was significantly lower than that in the SOD1-treated control 4 h after SCI (Fig. 3B).

PEP-1–SOD1 reduces motor neuron death

It is known that an increase in ROS stimulates the death of neurons after SCI [6,15]. Furthermore, motor neurons are selectively vulnerable to ROS and rapidly disappear early after SCI [12]. Therefore, we hypothesized that the PEP-1–SOD1 delivered exogenously would protect VMNs from ROS after SCI. A number of TUNEL-positive neurons in the ventral horn area were observed in the spinal cord after injury (Fig. 3C, SOD1 control), whereas no apoptotic neurons were found in the sham-operated spinal cord (Fig. 3C, sham). However, the number of TUNEL-positive neurons decreased when animals were injected with PEP-1–SOD1 after injury (Fig. 3C). Quantitative analysis of TUNEL-positive cells also showed that PEP-1–SOD1 treatment significantly decreased the number of TUNEL-positive apoptotic neurons in the ventral horn as compared with that observed in the SOD1-treated control 1 day after injury (Fig. 3D). DNA gel electrophoresis also revealed that PEP-1–SOD1 treatment markedly decreased DNA laddering when compared with the SOD1-treated control (Fig. 3E). To confirm the protective effect of PEP-1–SOD1 on VMNs after injury, serial transverse sections of the spinal cord were stained with cresyl violet, and VMNs were counted. A massive loss of VMNs was observed in the lesion area 4 days after injury (Fig. 4A, SOD1 control), as reported [11]. However, PEP-1–SOD1 treatment significantly reduced VMN loss in both the rostral and caudal regions from the lesion epicenter when compared with the SOD1 control, 4 days after injury (Figs. 4A and B).

PEP-1–SOD1 improves functional recovery after SCI

Locomotor function was examined to determine whether PEP-1–SOD1 fusion protein delivered exogenously improves functional

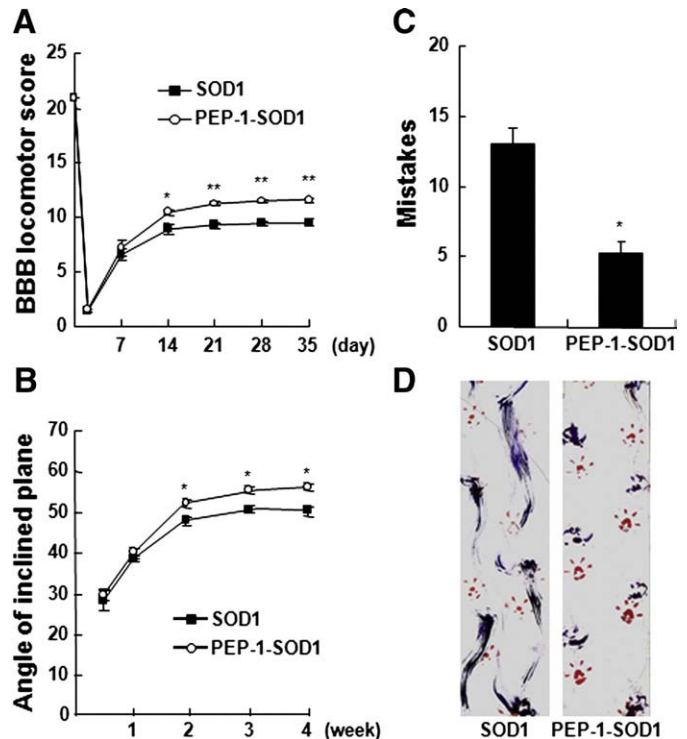


Fig. 5. PEP-1–SOD1 improves functional recovery after SCI. Functional recovery was assessed with the BBB scale, grid walk test, inclined plane test, and footprint analysis after injury. Each value represents the mean \pm SD obtained from 25 animals. (A) BBB scores of SOD1- and PEP-1–SOD1-treated groups after injury. * $P < 0.05$, ** $P < 0.01$. (B) Inclined plane test of SOD1- and PEP-1–SOD1-treated groups after injury. * $P < 0.05$. (C) Grid walk test of SOD1- and PEP-1–SOD1-treated groups 35 days after injury. * $P < 0.05$. (D) Representative footprints obtained from each group 35 days after SCI illustrate that PEP-1–SOD1-treated rats exhibited fairly consistent weight support plantar stepping and very little toe drag. By contrast, SOD1-treated (control) animals showed consistent dorsal stepping and extensive drag.

recovery after SCI. After injection of PEP-1–SOD1, functional recovery was assessed with the BBB locomotion scale, a standard method for assessing hindlimb locomotion in open fields [30]. The hindlimbs were paralyzed immediately after injury, and the rats recovered extensive movement of hindlimbs within 7 to 14 days after injury (Fig. 5A). As shown in Fig. 5A, PEP-1–SOD1 treatment after injury significantly increased hindlimb locomotor function, as assessed by BBB scores, 14 to 35 days after injury, as compared with the SOD1-

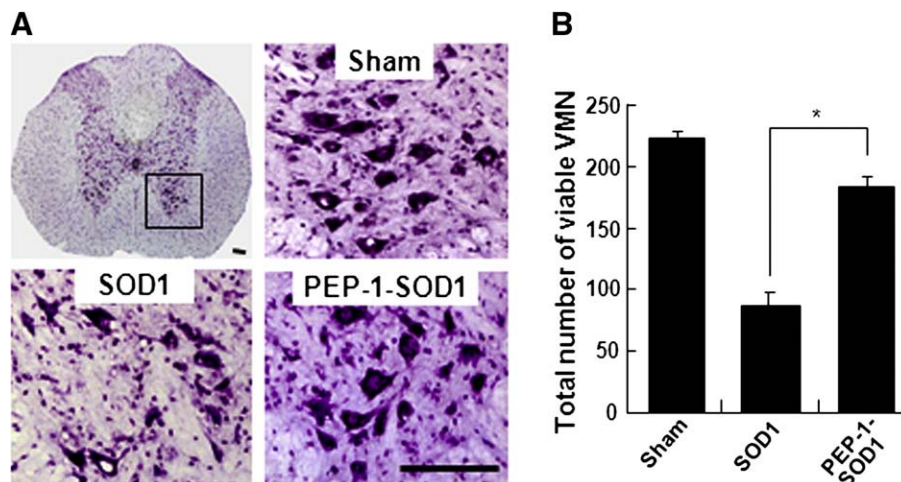


Fig. 4. PEP-1–SOD1 reduces the loss of viable motor neurons after SCI. (A) Ventral horn areas illustrated at low (inset, left, top panel) and higher powers. Representative sections were taken 2 mm rostral to the lesion epicenter 4 days after injury. Bar, 150 μ m. (B) For quantification, serial transverse sections (20 μ m thick) were collected every 500 μ m from 2.5 mm rostral to 2.5 mm caudal to the lesion epicenter (total of 11 sections) and neurons $> 30 \mu$ m in diameter were counted. Data represent the means \pm SD obtained from five separate experiments. ** $P < 0.001$.

treated control. The incline angles determined 1 to 4 weeks postinjury were also significantly higher in PEP-1-SOD1-treated animals than in SOD1-treated controls (Fig. 5B). The ability to control and place the hindlimbs precisely was tested on a horizontal grid 35 days after injury. The number of mistakes (footfalls on the grid walk) in the PEP-1-SOD1-treated group was significantly lower than that in the SOD1-treated group (Fig. 5C). Finally, in Fig. 5D are representative footprint recordings obtained from SOD1- and PEP-1-SOD1-treated rats 35 days after SCI. The footprints from the PEP-1-SOD1-treated rats showed fairly consistent weight support plantar stepping and very little toe

drag. By contrast, SOD1-treated animals showed consistent dorsal stepping and extensive drag as revealed by ink streaks extending from both hindlimbs.

PEP-1-SOD1 inhibits axon and tissue loss after SCI

Functional deficit after SCI was reported to be correlated with greater loss of axons in the white matter [40]. To examine whether PEP-1-SOD1 treatment would preserve axons after SCI, immunostaining using NF200 and 5-HT antibodies was performed to detect

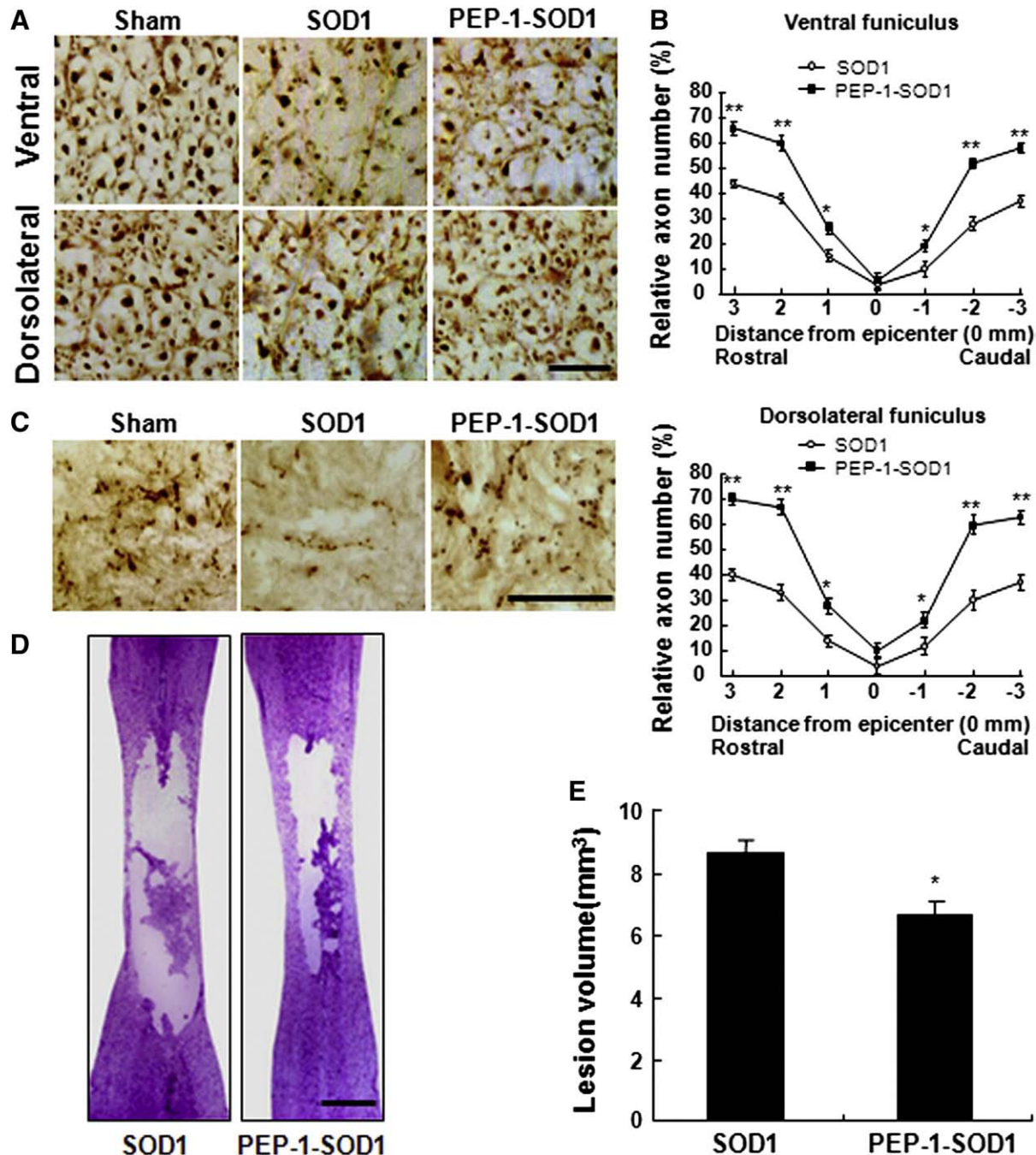


Fig. 6. PEP-1-SOD1 inhibits axon loss and reduces lesion volume after SCI. Transverse sections taken 2 mm rostral to the lesion epicenter 38 days after injury were processed for NF200 or 5-HT staining. (A) Representative photographs of NF200-positive axons in spinal cords. Sections were selected 2 mm rostral to the lesion site. Note that PEP-1-SOD1 treatment decreased the extent of axon loss after injury. Bar, 20 μ m. (B) Quantitative analysis of NF200-positive axons in ventral and dorsolateral funiculi showed that the density of spared axons in the PEP-1-SOD1-treated group was significantly higher than that in the SOD1-treated control. NF200-positive axons were counted as described under Materials and Methods. Data represent the means \pm SD obtained from five separate experiments. * P < 0.05, ** P < 0.01. (C) Representative photographs of 5-HT-positive axons in ventral horn areas at 3 mm caudal to lesion site. Bar, 40 μ m. (D) Representative spinal cord tissues (1.2 mm from dorsal surface) showing cavitation in the lesion site 38 days after injury. Bar, 1 mm. (E) Quantitative analysis of lesion volume 38 days after injury. Data represent the means \pm SD obtained from five separate experiments. * P < 0.05.

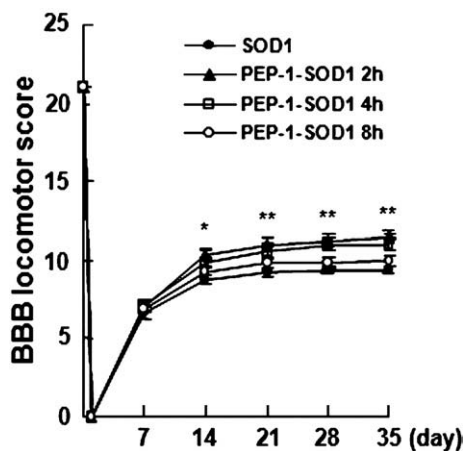


Fig. 7. Delayed administration of PEP-1-SOD1 improves functional recovery after SCI. PEP-1-SOD1 was administered 2, 4, or 8 h after injury, and functional recovery was assessed with the BBB scale ($n=12$). PEP-1-SOD1 treatment 2 or 4 h after injury significantly improved locomotor function when compared with the SOD1 control. * $P<0.05$, ** $P<0.01$.

remaining axons. Immunohistochemistry revealed that extensive axonal loss was observed at lesion sites after SCI (Fig. 6). In sham control animals, NF200-positive axons in the ventral and dorsolateral funiculi were dense and axonal packing was uniform (Fig. 6A, sham). Density of axons was markedly decreased and exhibited a patchy distribution in injured tissue 38 days after injury (Fig. 6A, SOD1). The numbers of NF200-positive axons in the ventral and dorsolateral funiculi were significantly higher in the PEP-1-SOD1-treated group than in the SOD1 control (Figs. 6A and B). Also, the density of serotonergic axons in the ventral horn was higher in PEP-1-SOD1-treated spinal cord than in SOD1-treated cord (Fig. 6C). Furthermore, lesion volume was significantly reduced by PEP-1-SOD1 treatment when compared with the SOD1 control, 38 days after injury (Figs. 6D and E).

Determination of therapeutic time window for administration of PEP-1-SOD1 after SCI

The time window for drug administration in acute SCI is a critical factor with respect to the possible therapeutic use of PEP-1-SOD1. To determine its therapeutic time window, PEP-1-SOD1 (1 mg/rat) was injected 2, 4, or 8 h after injury, and locomotor function was assessed with the BBB scale. As shown in Fig. 7, PEP-1-SOD1 treatment significantly improved BBB scores when it was injected 2 and 4 h after injury as compared with the SOD1 control. However, the BBB scores of rats injected 8 h after injury were not significantly different from those of the control.

Discussion

Peptide carriers are among the most promising tools for delivering biologically active molecules into cells; they have been shown to cross biological membranes efficiently, and to promote the delivery of peptides and proteins into cells in vitro and in vivo [21,41]. Recently, PEP-1, a short peptide carrier, has been shown to deliver proteins and peptides into several cell lines [42]. This peptide carrier presents several advantages for protein therapy, including its stability in physiological buffers, lack of toxicity, and lack of immunogenicity [42]. Furthermore, the mechanism through which PEP-1 delivers proteins does not involve the endosomal pathway [43]. Also, dissociation of the PEP-1/protein particle occurs immediately after it crosses the cell membrane [43].

Antioxidant enzymes including SOD1 have been considered as potential therapeutic agents for ALS, in which oxidative stress is

implicated in the death of motor neurons [16,17]. However, the lack of an efficient transduction system to deliver the enzymes into motor neurons has limited their use for protecting the neurons against oxidative stress. In the study described here, we demonstrated that the PEP-1-SOD1 fusion protein is delivered efficiently into cultured neurons and injured spinal cord in a biologically active form. We also showed that the intracellular stability of the fusion protein persisted for 24 h (see Fig. 1D). Furthermore, systemic administration of the fusion protein protected motor neurons from ROS and thereby improved recovery after SCI. These results indicate that PEP-1 technology could be extremely useful for developing therapeutic applications for central nervous system injury that include SCI, as well as for such neurodegenerative diseases as ALS.

Although SOD at high concentrations is potentially toxic to cells [44], no adverse effects such as weight loss and immune response were observed at the dose of PEP-1-SOD1 (1 mg/rat) used in the present study. Furthermore, PEP-1 has no toxicity at concentrations up to 100 μM in various cell lines [42]. A previous study demonstrated that PEP-1-SOD1 fusion proteins effectively protect against neuronal cell damage caused by ischemic insult and that 4 mg/kg is an optimal dose for neuroprotection in gerbils [22]. Also, among the various doses of PEP-1-SOD1 administered in this study, 1 mg/rat led to the highest functional recovery after SCI (data not shown).

ROS have been shown to produce immediate functional losses, progressive tissue degeneration, and neuronal death after SCI [9,16,45]. The present study showed that after SCI, ROS such as O_2^- are generated rapidly and stimulate apoptosis of neurons, particularly VMNs. Previously, we reported that nitric oxide is also produced early after SCI and induces apoptosis of neurons after SCI [4]. Together, these data suggest that ROS may play a pivotal role in the apoptotic cell death of neurons including VMNs after SCI.

Oxidative stress-induced membrane damage results in the loss of membrane fluidity by lipid peroxidation, thereby destroying the integrity of the cell membrane [46]. Also, oxidation of proteins is generally accepted as a major pathogenic mechanism of oxidative stress, and this phenomenon has been well studied in aging and in cerebral ischemia [47,48]. The carbonylation of proteins is a result of oxidative damage and is considered an indicator of severe oxidative damage and disease-derived protein dysfunction [35,36]. A number of neurodegenerative diseases have been associated with the accumulation of proteolysis-resistant aggregates of carbonylated proteins in tissues [49,50]. For example, elevated levels of protein carbonyls are found in the brains of persons with mild cognitive impairment, a condition that often precedes Alzheimer's disease, suggesting that oxidative damage may be among the earliest events in the onset and progression of Alzheimer's disease [51]. Our results indicate that protein carbonylation is dramatically increased after SCI and that PEP-1-SOD1 treatment significantly attenuates the extent of this protein carbonylation. After SCI, the levels of NO also increase, and peroxynitrite is formed when NO reacts with O_2^- [4,5]. Peroxynitrite is known to mediate several destructive chemical reactions, including protein nitration and lipid peroxidation [52]. Our data also demonstrate that the level of protein nitration increases and VMNs become positive for nitrotyrosine after SCI. Furthermore, PEP-1-SOD1 treatment significantly decreases the level of protein nitration in VMNs. Thus, these data suggest that exogenously administered PEP-1-SOD1 scavenges ROS and thus inhibits protein nitration and carbonylation in VMNs after SCI.

Our results indicate that PEP-1-SOD1 treatment can improve functional recovery after SCI. The hindlimbs were paralyzed immediately after injury, and animals in both the SOD1 control and PEP-1-SOD1 treated groups recovered extensive movement of hindlimbs within 7 to 14 days after injury (see Fig. 5A). However, the differences in BBB scores between the SOD1 control and PEP-1-SOD1 groups were evident at 14 to 35 days after injury. The BBB score provides information on local spinal pattern generating networks that regulate

coordinated stepping [30,53,54]. It is known that significant sparing of axons within the ventral and dorsolateral funiculi (which contain the vestibulospinal tract and rubrospinal tract, respectively) is related to stepping abilities and overground locomotion [55]. Our data also show that the density of spared axons within the ventral and dorsolateral funiculi was higher in the PEP-1–SOD1-treated group than in the SOD1 control group (see Fig. 6A). These observations agree with the inclined plane scores in Fig. 5B, as the integrity of the nonpyramidal tracts, in particular the rubrospinal tracts, vestibulospinal tracts, and raphespinal tracts, is highly correlated with inclined plane performance in spinal cord-injured rats [56]. The grid walk scores indicate deficits in the descending pathways for fine motor control after SCI [57,58]. Fig. 5C shows that the number of footfalls (mistakes) was lower than that of the SOD1 control group, suggesting fine motor control was significantly improved by PEP-1–SOD1 treatment. Furthermore, we showed that PEP-1–SOD1 treatment reduced degeneration of 5-HT-positive serotonergic fibers in the ventral horn, whereas extensive degeneration of serotonergic fibers was observed in the SOD1-treated spinal cord (Fig. 6C). These serotonergic fibers are correlated with locomotor function as 5-HT is one of the key neurotransmitters responsible for initiating locomotion [59].

In summary, we demonstrated for the first time that the PEP-1–SOD1 fusion protein is delivered both efficiently and in a biologically active form into injured spinal cords in vivo. Systemically injected PEP-1–SOD1 decreased the levels of ROS in VMNs, inhibited the apoptotic cell death of VMNs, and thereby improved functional recovery after SCI. Thus, our data suggest that PEP-1–SOD1 may provide a new strategy for the therapeutic delivery of antioxidant enzymes for treatment of SCI.

Acknowledgments

The authors thank Dr. George Markelonis at the University of Maryland School of Medicine for his editorial assistance. The authors thank Dr. Kwon I. C. at Korea Institute of Science and Technology for technical assistance (in situ detection of superoxide anion). This study was supported in part by a Korea Science and Engineering Foundation (KOSEF) grant funded by the Korean government (MOST) (No. R01-2007-000-20617-0, M1041200011-07N1200-01110), the Seoul R&BD Program (No. 10524), the Post BK21 Program, and Kyung Hee University.

References

- [1] Crowe, M. J.; Bresnahan, J. C.; Shuman, S. L.; Masters, J. N.; Beattie, M. S. Apoptosis and delayed degeneration after spinal cord injury in rats and monkeys. *Nat. Med.* **3**:73–76; 1997.
- [2] Springer, J. E.; Azbill, R. D.; Knapp, P. E. Activation of the caspase-3 apoptotic cascade in traumatic spinal cord injury. *Nat. Med.* **5**:943–946; 1999.
- [3] Lewen, A.; Matz, P.; Chan, P. H. Free radical pathways in CNS injury. *J. Neurotrauma* **17**:871–890; 2000.
- [4] Yune, T. Y.; Chang, M. J.; Kim, S. J.; Lee, Y. B.; Shin, S. W.; Rhim, H.; Kim, Y. C.; Shin, M. L.; Oh, Y. J.; Han, C. T.; Markelonis, G. J.; Oh, T. H. Increased production of tumor necrosis factor- α induces apoptosis after traumatic spinal cord injury in rats. *J. Neurotrauma* **20**:207–219; 2003.
- [5] Bao, F.; Liu, D. Peroxynitrite generated in the rat spinal cord induces neuron death and neurological deficits. *Neuroscience* **115**:839–849; 2002.
- [6] Bao, F.; Liu, D. Hydroxyl radicals generated in the rat spinal cord at the level produced by impact injury induce cell death by necrosis and apoptosis: protection by a metalloporphyrin. *Neuroscience* **126**:285–295; 2004.
- [7] Facchinetti, F.; Dawson, V. L.; Dawson, T. M. Free radicals as mediators of neuronal injury. *Cell Mol. Neurobiol.* **18**:667–682; 1998.
- [8] Juurlink, B. H.; Paterson, P. G. Review of oxidative stress in brain and spinal cord injury: suggestions for pharmacological and nutritional management strategies. *J. Spinal Cord Med.* **21**:309–334; 1998.
- [9] Liu, D.; Liu, J.; Wen, J. Elevation of hydrogen peroxide after spinal cord injury detected by using the Fenton reaction. *Free Radic. Biol. Med.* **27**:478–482; 1999.
- [10] Fujimura, M.; Morita-Fujimura, Y.; Murakami, K.; Kawase, M.; Chan, P. H. Cytosolic redistribution of cytochrome c after transient focal cerebral ischemia in rats. *J. Cereb. Blood Flow Metab.* **18**:1239–1247; 1998.
- [11] Sugawara, T.; Lewen, A.; Gasche, Y.; Yu, F.; Chan, P. H. Overexpression of SOD1 protects vulnerable motor neurons after spinal cord injury by attenuating mitochondrial cytochrome c release. *FASEB J.* **16**:1997–1999; 2002.
- [12] Grossman, S. D.; Rosenberg, L. J.; Wrathall, J. R. Temporal-spatial pattern of acute neuronal and glial loss after spinal cord contusion. *Exp. Neurol.* **168**:273–282; 2001.
- [13] Tomiyama, M.; Kimura, T.; Maeda, T.; Tanaka, H.; Furusawa, K.; Kurahashi, K.; Matsunaga, M. Expression of metabotropic glutamate receptor mRNAs in the human spinal cord: implications for selective vulnerability of spinal motor neurons in amyotrophic lateral sclerosis. *J. Neurol. Sci.* **189**:65–69; 2001.
- [14] Wengenack, T. M.; Holasek, S. S.; Montano, C. M.; Gregor, D.; Curran, G. L.; Poduslo, J. F. Activation of programmed cell death markers in ventral horn motor neurons during early presymptomatic stages of amyotrophic lateral sclerosis in a transgenic mouse model. *Brain Res.* **1027**:73–86; 2004.
- [15] Xu, W.; Chi, L.; Xu, R.; Ke, Y.; Luo, C.; Cai, J.; Qiu, M.; Gozal, D.; Liu, R. Increased production of reactive oxygen species contributes to motor neuron death in a compression mouse model of spinal cord injury. *Spinal Cord* **43**:204–213; 2005.
- [16] Liu, D.; Sybert, T. E.; Qian, H.; Liu, J. Superoxide production after spinal injury detected by microperfusion of cytochrome c. *Free Radic. Biol. Med.* **25**:298–304; 1998.
- [17] Guegan, C.; Vila, M.; Rosoklija, G.; Hays, A. P.; Przedborski, S. Recruitment of the mitochondrial-dependent apoptotic pathway in amyotrophic lateral sclerosis. *J. Neurosci.* **21**:6569–6576; 2001.
- [18] Vives, E. G.; Brodin, P.; Lebleu, B. A truncated HIV-1 Tat protein basic domain rapidly translocates through the plasma membrane and accumulates in the cell nucleus. *J. Biol. Chem.* **272**:16010–16017; 1997.
- [19] Fawell, N. G.; Cookson, T. L.; Scranton, S. S. Relationship between tablet splitting and compliance, drug acquisition cost, and patient acceptance. *Am. J. Health Syst. Pharm.* **56**:2542–2545; 1999.
- [20] Prochiantz, A. Messenger proteins: homeoproteins, TAT and others. *Curr. Opin. Cell Biol.* **12**:400–406; 2000.
- [21] Morris, M. C.; Chaloin, L.; Heitz, F.; Divita, G. Translocating peptides and proteins and their use for gene delivery. *Curr. Opin. Biotechnol.* **11**:461–466; 2000.
- [22] Eum, W. S.; Kim, D. W.; Hwang, I. K.; Yoo, K. Y.; Kang, T. C.; Jang, S. H.; Choi, H. S.; Choi, S. H.; Kim, Y. H.; Kim, S. Y.; Kwon, H. Y.; Kang, J. H.; Kwon, O. S.; Cho, S. W.; Lee, K. S.; Park, J.; Won, M. H.; Choi, S. Y. In vivo protein transduction: biologically active intact pep-1–superoxide dismutase fusion protein efficiently protects against ischemic insult. *Free Radic. Biol. Med.* **37**:1656–1669; 2004.
- [23] Choi, H. S.; An, J. J.; Kim, S. Y.; Lee, S. H.; Kim, D. W.; Yoo, K. Y.; Won, M. H.; Kang, T. C.; Kwon, H. J.; Kang, J. H.; Cho, S. W.; Kwon, O. S.; Park, J.; Eum, W. S.; Choi, S. Y. PEP-1–SOD fusion protein efficiently protects against paraquat-induced dopaminergic neuron damage in a Parkinson disease mouse model. *Free Radic. Biol. Med.* **41**:1058–1068; 2006.
- [24] Yune, T. Y.; Kim, S. J.; Lee, S. M.; Lee, Y. K.; Oh, Y. J.; Kim, Y. C.; Markelonis, G. J.; Oh, T. H. Systemic administration of 17 β -estradiol reduces apoptotic cell death and improves functional recovery following traumatic spinal cord injury in rats. *J. Neurotrauma* **21**:293–306; 2004.
- [25] Lee, S. M.; Yune, T. Y.; Kim, S. J.; Kim, Y. C.; Oh, Y. J.; Markelonis, G. J.; Oh, T. H. Minocycline inhibits apoptotic cell death via attenuation of TNF- α expression following iNOS/NO induction by lipopolysaccharide in neuron/glia co-cultures. *J. Neurochem.* **91**:568–578; 2004.
- [26] Yune, T. Y.; Lee, S. M.; Kim, S. J.; Park, H. K.; Oh, Y. J.; Kim, Y. C.; Markelonis, G. J.; Oh, T. H. Manganese superoxide dismutase induced by TNF- α is regulated transcriptionally by NF- κ B after spinal cord injury in rats. *J. Neurotrauma* **21**:1778–1794; 2004.
- [27] Bindokas, V. P.; Jordan, J.; Lee, C. C.; Miller, R. J. Superoxide production in rat hippocampal neurons: selective imaging with hydroethidine. *J. Neurosci.* **16**:1324–1336; 1996.
- [28] Kondo, T.; Reaume, A. G.; Huang, T. T.; Carlson, E.; Murakami, K.; Chen, S. F.; Hoffman, E. K.; Scott, R. W.; Epstein, C. J.; Chan, P. H. Reduction of CuZn-superoxide dismutase activity exacerbates neuronal cell injury and edema formation after transient focal cerebral ischemia. *J. Neurosci.* **17**:4180–4189; 1997.
- [29] Carter, W. O.; Narayanan, P. K.; Robinson, J. P. Intracellular hydrogen peroxide and superoxide anion detection in endothelial cells. *J. Leukoc. Biol.* **55**:253–258; 1994.
- [30] Yu, C. G.; Geddes, J. W. Sustained calpain inhibition improves locomotor function and tissue sparing following contusive spinal cord injury. *Neurochem. Res.* **32**:2046–2053; 2007.
- [31] Basso, D. M.; Beattie, M. S.; Bresnahan, J. C. A sensitive and reliable locomotor rating scale for open field testing in rats. *J. Neurotrauma* **12**:1–21; 1995.
- [32] Rivlin, A. S.; Tator, C. H. Objective clinical assessment of motor function after experimental spinal cord injury in the rat. *J. Neurosurg.* **47**:577–581; 1977.
- [33] Merkle, D.; Metz, G. A.; Raineteau, O.; Dietz, V.; Schwab, M. E.; Fouad, K. I. Locomotor recovery in spinal cord-injured rats treated with an antibody neutralizing the myelin-associated neurite growth inhibitor Nogo-A. *J. Neurosci.* **21**:3665–3673; 2001.
- [34] Stirling, D. P.; Khodarahmi, K.; Liu, J.; McPhail, L. T.; McBride, C. B.; Streeves, J. D.; Ramer, M. S.; Tetzlaff, W. Minocycline treatment reduces delayed oligodendrocyte death, attenuates axonal dieback, and improves functional outcome after spinal cord injury. *J. Neurosci.* **24**:2182–2190; 2004.
- [35] Valko, M.; Leibfritz, D.; Moncol, J.; Cronin, M. T.; Mazur, M.; Telsler, J. Free radicals and antioxidants in normal physiological functions and human disease. *J. Biochem. Cell Biol.* **39**:44–84; 2007.
- [36] Berlett, B. S.; Stadtman, E. R. Protein oxidation in aging, disease, and oxidative stress. *J. Biol. Chem.* **272**:20313–20316; 1997.
- [37] Dalle-Donne, I.; Aldini, G.; Carini, M.; Colombo, R.; Rossi, R.; Milzani, A. Protein carbonylation, cellular dysfunction, and disease progression. *J. Cell. Mol. Med.* **10**:389–406; 2006.
- [38] Springer, J. E.; Azbill, R. D.; Knapp, P. E. Activation of the caspase-3 apoptotic cascade in traumatic spinal cord injury. *Nat. Med.* **5**:943–946; 1999.
- [39] Citron, B. A.; Arnold, P. M.; Sebastian, C.; Qin, F.; Malladi, S.; Ameenuddin, S.; Landis, M. E.; Festoff, B. W. Rapid upregulation of caspase-3 in rat spinal cord after

- injury: mRNA, protein, and cellular localization correlates with apoptotic cell death. *Exp. Neurol.* **166**:213–226; 2000.
- [40] Basso, D. M.; Beattie, M. S.; Bresnahan, J. C.; Anderson, D. K.; Faden, A. I.; Gruner, J. A.; Holford, T. R.; Hsu, C. Y.; Noble, L. J.; Nockels, R.; Perot, P. L.; Salzman, S. K.; Young, W. MASCIS evaluation of open field locomotor scores: effects of experience and teamwork on reliability. Multicenter Animal Spinal Cord Injury Study. *J. Neurotrauma* **13**:343–359; 1996.
- [41] Wadia, J. S.; Dowdy, S. F. Protein transduction technology. *Curr. Opin. Biotechnol.* **13**:52–56; 2002.
- [42] Morris, M. C.; Depollier, J.; Mery, J.; Heitz, F.; Divita, G. A. A peptide carrier for the delivery of biologically active proteins into mammalian cells. *Nat. Biotechnol.* **19**:1173–1176; 2001.
- [43] Gros, E.; Deshayes, S.; Morris, M. C.; Aldrian-Herrada, G.; Depollier, J.; Heitz, F.; Divita, G. A non-covalent peptide-based strategy for protein and peptide nucleic acid transduction. *Biochim. Biophys. Acta* **1758**:384–393; 2006.
- [44] Mao, G. D.; Thomas, P. D.; Lopaschuk, G. D.; Poznansky, M. J. Superoxide dismutase (SOD)–catalase conjugates: role of hydrogen peroxide and the Fenton reaction in SOD toxicity. *J. Biol. Chem.* **268**:416–420; 1993.
- [45] Mu, X.; Azbill, R. D.; Springer, J. E. NBQX treatment improves mitochondrial function and reduces oxidative events after spinal cord injury. *J. Neurotrauma* **19**:917–927; 2002.
- [46] Subramaniam, R.; Roediger, F.; Jordan, B.; Mattson, M. P.; Keller, J. N.; Waeg, G.; Butterfield, D. A. The lipid peroxidation product, 4-hydroxy-2-trans-nonenal, alters the conformation of cortical synaptosomal membrane proteins. *J. Neurochem.* **69**:1161–1169; 1997.
- [47] Dubey, A.; Forster, M. J.; Sohal, R. S. Effect of the spin-trapping compound *N*-tert-butyl-alpha-phenylnitron on protein oxidation and life span. *Arch. Biochem. Biophys.* **324**:249–254; 1995.
- [48] Hall, N. C.; Dempsey, R. J.; Carney, J. M.; Donaldson, D. L.; Butterfield, D. A. Structural alterations in synaptosomal membrane-associated proteins and lipids by transient middle cerebral artery occlusion in the cat. *Neurochem. Res.* **20**:1161–1169; 1995.
- [49] Choi, J.; Forster, M. J.; McDonald, S. R.; Weintraub, S. T.; Carroll, C. A.; Gracy, R. W. Proteomic identification of specific oxidized proteins in ApoE-knockout mice: relevance to Alzheimer's disease. *Free Radic. Biol. Med.* **36**:1155–1162; 2004.
- [50] Jiang, H.; Ren, Y.; Zhao, J.; Feng, J. Parkin protects human dopaminergic neuroblastoma cells against dopamine-induced apoptosis. *Hum. Mol. Genet.* **13**:1745–1754; 2004.
- [51] Keller, J. N.; Schmitt, F. A.; Scheff, S. W.; Ding, Q.; Chen, Q.; Butterfield, D. A.; Markesbery, W. R. Evidence of increased oxidative damage in subjects with mild cognitive impairment. *Neurology* **64**:1152–1156; 2005.
- [52] Szabo, C. Multiple pathways of peroxynitrite cytotoxicity. *Toxicol. Lett.* **140–141**:105–112; 2003.
- [53] Grillner, S. Neural networks for vertebrate locomotion. *Sci. Am.* **274**:64–69; 1996.
- [54] Jordan, L. M. Initiation of locomotion in mammals. *Ann. NY Acad. Sci.* **860**:83–93; 1998.
- [55] Schucht, P.; Raineteau, O.; Schwab, M. E.; Fouad, K. Anatomical correlates of locomotor recovery following dorsal and ventral lesions of the rat spinal cord. *Exp. Neurol.* **176**:143–153; 2002.
- [56] Fehlings, M. G.; Tator, C. H. The relationships among the severity of spinal cord injury, residual neurological function, axon counts, and counts of retrogradely labeled neurons after experimental spinal cord injury. *Exp. Neurol.* **132**:220–228; 1995.
- [57] Kunkel-Bagden, E.; Hai-Ning, D.; Bregman, B. S. Methods to assess the development and recovery of locomotor function after spinal cord injury in rats. *Exp. Neurol.* **119**:153–164; 1993.
- [58] Metz, G. A.; Merkler, D.; Dietz, V.; Schwab, M. E.; Fouad, K. Efficient testing of motor function in spinal cord injured rats. *Brain Res.* **883**:165–177; 2000.
- [59] Saruhashi, Y.; Young, W.; Perkins, R. The recovery of 5-HT immunoreactivity in lumbosacral spinal cord and locomotor function after thoracic hemisection. *Exp. Neurol.* **139**:203–213; 1996.